Applied Catalysis B: Environmental 117–118 (2012) 212–223

Contents lists available at SciVerse ScienceDirect

Applied Catalysis B: Environmental

journal homepage: www.elsevier.com/locate/apcatb

The SCR of NO with methane over In,H- and Co,In,H-ZSM-5 catalysts: The promotional effect of cobalt

Ferenc Lónyi[a,*], Hanna E. Solt[a], József Valyon[a], Alicia Boix[b], Laura B. Gutierrez[b]

[a] Institute of Nanochemistry and Catalysis, Chemical Research Center, Hungarian Academy of Sciences, Pusztaszeri u. 59-67, 1025 Budapest, Hungary
[b] Instituto de Investigaciones en Catálisis y Petroquimica, INCAPE (FIQ, UNL-CONICET), Santiago del Estero 2829, 3000 Santa Fe, Argentina

ARTICLE INFO

Article history:
Received 10 November 2011
Received in revised form 13 January 2012
Accepted 18 January 2012
Available online 28 January 2012

Keywords:
In,H-ZSM-5
Promotion by Co
NO-SCR by CH_4
Operando DRIFTS

ABSTRACT

Zeolite In,H-, Co,H-, and Co,In,H-ZSM-5 were characterized by operando diffuse reflectance infrared Fourier transform spectroscopy (DRIFTS), temperature-programmed reduction by hydrogen (H_2-TPR), X-ray photoelectron spectroscopy (XPS), and activity in the selective catalytic reduction of NO (NO-SCR) by methane. The catalysts were shown to contain indium as $[InO]^+/[InOH]^{2+}$ cations, whereas cobalt was in the form of $Co^{2+}/[Co\text{-}OH]^+$ cations or Co-oxide clusters in amounts controlled by the applied preparation method. The NO-SCR by methane was shown to proceed in two coupled processes on distinctly different catalytic sites. One of the processes is the oxidation of NO to NO_2 by oxygen over Brønsted acid sites and/or cobalt-oxide species giving NO/NO_2 gas mixture (NO-COX reaction). The other process is the N_2 formation, which is the result of the reaction of methane and the NO/NO_2 mixture (CH_4/NO-SCR reaction). Molecules of NO and NO_2 were shown to become activated together as NO^+/NO_3^- ion pair in reaction with $[InO]^+/[InOH]^{2+}$ or $Co^{2+}/[Co\text{-}OH]^+$ sites. Operando DRIFTS results suggested that the reaction of methane and NO_3^- generates an intermediate that rapidly reacts with the NO^+ to give N_2. The promoting effect of the cobalt was related to the significantly higher NO-COX activity of Co-oxide clusters than that of the Brønsted acid sites. The accelerated NO-COX reaction speeds up the formation of NO^+/NO_3^- species and the rate of the methane activation, being the rate-determining step of the NO-SCR reaction. It was also shown that the NO-SCR reaction can proceed if NO-COX and CH_4/NO-SCR active sites are separated in space. In order to avoid rate controlling NO_2 transport between the sites close proximity of the sites is favorable.

1. Introduction

For the abatement of nitrogen oxides (NO_x) from O_2-rich emissions the selective catalytic reduction (NO-SCR) by hydrocarbon is a promising technology [1–4]. The use of cheap and abundantly available methane as reducing agent can be especially beneficial to control the NO_x emission of boilers and engines fueled by natural gas [3,5–7]. However, the activation of methane for the reduction of NO is difficult. Only a few metal-based catalysts such as supported Pt, Pd, Co, Mn, Ni, Ga and In (and their combinations) show substantial activity [3,4].

Indium-zeolites were among the most studied catalytic systems [8–24]. Their activity could be increased by a wide variety of promoters including transition metals such as Ir [10], Pt [12,22], Pd [22], or Co [20,21], and finely dispersed metal oxides, such as CeO_x [14,24], colloidal Al_2O_3 [15], In_2O_3 [17], Fe_xO_y [19], and Mn_3O_4 [22]. These promoters not only enhanced the activity of In-zeolites, but also improved their water tolerance, which is a key issue of practical application.

It is generally accepted that $[InO]^+$ cations in ion-exchange positions are responsible for the NO-SCR activity of the In-zeolites [8–10,12–14,16,17,19,21], whereas the promoters are believed to help the reaction by facilitating the oxidation of NO to NO_2 by oxygen (NO-COX reaction) [10,12,14,15,17,19–22]. The NO_2, being a better oxidant than NO, can efficiently compete with O_2 for the oxidation of methane. Recent studies suggested that the reactions of NO_2 and the N_2 generation (NO-COX and CH_4/NO-SCR reactions) proceed on different active sites. It was possible to get high NO-SCR activity by mixing two catalysts: one having high NO-COX activity and another, active in the CH_4/NO-SCR reaction [7,8,22,24–27].

The cobalt was found to be one of the best promoters [20,21]. It was suggested to be present as extra-framework Co^{2+}, $[Co\text{-}OH]^+$, or Co^{3+} cation or as finely dispersed Co-oxide, such as CoO and/or Co_3O_4, within the zeolite pores or on the outer surface of the zeolite crystallites [21,28–33]. Recent studies suggested that the promoting effect appeared due to synergism of Co^{2+} and $[InO]^+$ sites [20,21]. Kubacka et al. [21] attributed the promoting effect

* Corresponding author. Tel.: +36 1 438 1162; fax: +36 1 438 1164.
E-mail address: lonyi@chemres.hu (F. Lónyi).

0926-3373/$ – see front matter © 2012 Elsevier B.V. All rights reserved.
doi:10.1016/j.apcatb.2012.01.022

Table 1
Catalyst preparations and composition.

Catalyst Sample	Preparation method	Al_F/In	Al_F/Co
In,H-ZSM-5	RSSIE[a]	0.33	–
Co^{IE},H-ZSM-5	IE[b]	–	0.125
Co^{SSR},H-ZSM-5	SSR[c]	–	0.125
In,Co^{IE},H-ZSM-5	1st Co by IE 2nd In by RSSIE	0.33	0.125
In,Co^{SSR},H-ZSM-5	1st Co by SSR 2nd In by RSSIE	0.33	0.125
Co^{SSR},In,H-ZSM-5	1st In by RSSIE 2nd Co by SSR	0.33	0.125

[a] Reductive solid state ion-exchange.
[b] Liquid phase ion-exchange.
[c] Solid state reaction.

to isolated Co^{2+} ions, whereas Co-oxide species and particularly Co_3O_4 aggregates were believed to be responsible for the undesired methane oxidation with O_2 [21,32]. In contrast, Traa et al. [3] found that cobalt oxide particles promote the NO-COX reaction and assumed to facilitate the NO-SCR reaction just like any of the above-mentioned promoters. One can also assume that the promoter increases somehow the NO-COX activity of the Brønsted acid sites. Some authors, detecting NO_2 as product, strongly questioned that NO_2 could be active intermediate of the NO-SCR reaction [30,31].

Many studies substantiated that the NO-COX activity was a crucial function of the NO-SCR catalyst, however, the role of NO_2 in the reaction is not fully understood yet. It is not clear how the increased rate of the NO-COX reaction, accelerated by promoter, increases the rate of the NO-SCR by methane. Neither the Co species, having promotional effect in the Co,In,H-zeolites, nor the promoting mechanism are known. In the present study we give plausible explanation for above questions.

2. Experimental

2.1. Catalyst preparation

The In,H-ZSM-5 sample was prepared by the method of reductive solid state ion exchange (RSSIE). H-ZSM-5 (our synthetic product; $Si/Al_T = 29.7$ and $Si/Al_F = 33.0$, where Al_T and Al_F represent the total and the framework aluminum content, respectively) were mixed with In_2O_3 (Aldrich; 99.99%) applying intense co-grinding. The obtained In_2O_3/H-zeolite mixtures were treated in H_2 flow at 773 K for 1 h, then cooled down to room temperature in He flow and finally oxidized in O_2 flow at 673 K. The In/Al_F ratio of the ZSM-5 catalyst was 0.33 (1.7 wt% In content).

Two different methods were applied to prepare Co,H-ZSM-5 samples, such as liquid phase ion-exchange (IE) or solid state reaction (SSR). The IE was carried out by stirring 10 g of H-ZSM-5 sample in 500 ml of a 0.1 M $Co(NO_3)_2$ solution at 343 K under reflux for 6 h. Then the slurry was filtered, washed with distilled water and dried in an oven at 383 K. The ion-exchanged sample was designated as Co^{IE},H-ZSM-5 and the Co/Al_F ratio in the sample was 0.125 (0.34 wt% Co content, determined by chemical analysis). A Co-zeolite sample containing the same amount of Co was prepared by reacting the H-ZSM-5 sample with a calculated amount of $Co(CH_3COO)_2{\cdot}4H_2O$ in the solid state. A similar procedure was applied than that described in Refs. [20] and [21]. The zeolite and cobalt acetate powders were mixed by intense co-grinding. The mixture was heated up to 823 K at a heating rate of 10 K min^{-1} to 823 K in a He flow (30 cm^3 min^{-1}) and kept at this temperature for 2 h. The sample prepared by the above outlined SSR method was designated as Co^{SSR},H-ZSM-5.

Catalyst samples containing both In and Co were prepared from an aliquot part of the Co^{IE},H-ZSM-5 and Co^{SSR},H-ZSM-5 samples by introducing the same amount of In as was in the In,H-ZSM-5 sample ($In/Al_F = 0.33$) using the RSSIE method. These samples were designated as In,Co^{IE},H-ZSM-5 and In,Co^{SSR},H-ZSM-5, respectively. An additional bimetallic sample was prepared from an aliquot part of the In,H-ZSM-5 sample by introducing the same amount of Co as was in the Co,H-ZSM-5 samples by the SSR method. This sample was denoted as Co^{SSR},In,H-ZSM-5. Note that the In,Co^{SSR},H- and the Co^{SSR},In,H-preparations differ in the order of metal introduction. The various catalyst preparations and their compositions are listed in Table 1.

2.2. Temperature-programmed reduction by hydrogen (H_2-TPR)

Curves of H_2-TPR were measured using a flow-through microreactor (I.D. 4 mm) made of quartz. About 150 mg of catalyst sample (particle size: 0.25–0.5 mm) was placed into the microreactor and was pretreated in a 30 cm^3 min^{-1} flow of O_2 at 773 K for 1 h before the H_2-TPR measurement. The pre-treated sample was purged with N_2 at 773 K and cooled to room temperature in the same N_2 flow then was contacted with a 30 cm^3 min^{-1} flow of 10% H_2/N_2 mixture. The reactor temperature was ramped up at a rate of 10 K min^{-1} to 1073 K, while the effluent gas was passed through a dry-ice trap and a thermal conductivity detector (TCD). Data were collected and processed by computer. Calculation of the corresponding hydrogen consumptions based on the peak areas was carried out by using the calibration value determined with the H_2-TPR of CuO reference material.

2.3. X-ray photoelectron spectroscopy (XPS)

XPS analyses were performed in a multi-technique system (SPECS) equipped with a dual Mg/Al X-ray source and a hemispherical PHOIBOS 150 analyzer operating in the fixed analyzer transmission (FAT) mode. Each catalyst sample was pretreated *ex situ* in a 30 cm^3 min^{-1} flow of O_2 at 773 K for 1 h before the XPS experiments. The pellet, pressed from the pretreated catalyst powder, was placed into the reaction chamber of the XPS apparatus and was pretreated *in situ* in vacuum at 673 K for 1 h then cooled to room temperature. The spectra were obtained with pass energy of 30 eV; an Al-Kα X-ray source was operated at 200 W and 12 kV. The working pressure in the analyzing chamber was less than 5×10^{-9} mbar. The spectral regions corresponding to In 3d, Co 2p, O 1s, C 1s, Si 2p, Si 2s and Al 2p core levels were recorded for each sample. The BE reference value was $Si_{2p} = 103.0$ eV. The data treatment was performed with the Casa XPS program (Casa Software Ltd., UK). The peak areas were determined by integration employing a Shirley-type background. Peaks were considered to be a mixture of Gaussian and Lorentzian functions in a 70/30 ratio. For the quantification of the elements, sensitivity factors provided by the manufacturer were used.

2.4. Catalytic activity

The same flow-through microreactor was used as for the H_2-TPR measurements. Usually about 100 mg of catalyst (particle size: 0.25–0.5 mm) was pre-treated in a 30 cm^3 min^{-1} flow of 10%O_2/He at 773 K for 1 h, then the sample was purged with pure He and cooled to 573 K. The catalytic activities in the selective catalytic reduction (NO-SCR) and in the catalytic oxidation of NO to NO_2 with O_2 (NO-COX) were determined at temperatures between 573 and 873 K. The reaction was initiated by switching the He flow to a flow of 4000 ppm NO/4000 ppm CH_4/2% O_2/He mixture (NO-SCR) or 4000 ppm NO/2% O_2/He mixture (NO-COX). From here on these gas mixtures are referred to as NO/CH_4/O_2 or NO/O_2 mixtures without giving the concentrations and indicating the presence of helium. The total flow rate of the reaction mixture was 100 cm^3 min^{-1} throughout the catalytic experiments corresponding to about a GHSV value of 30 000 h^{-1}. (The bed volume was calculated using catalyst bulk density of 0.5 g cm^{-3}). The reactor effluent was analyzed with an on-line MS (VG ProLab, Fisher Scientific) having a computer program for a quantitative analysis. The instrument was calibrated using gas mixtures with known compositions. The composition of the reactor effluent was continuously monitored. The total conversions in the NO-SCR reaction were calculated as follows:

$$\text{Total conversion of NO (mol\%)} = \frac{[NO]^0 - [NO]}{[NO]^0} \times 100$$

In order to circumvent the uncertainty coming from the overlapping $m/z = 28$ MS signal of N_2 and CO the conversion to N_2 was calculated by the equation below.

$$\text{Conversion of NO to } N_2\text{ (mol\%)} = \frac{[NO]^0 - [NO] - [NO_2] - 2[N_2O]}{[NO]^0} \times 100$$

In the equations $[NO]^0$ stands for the initial concentration of NO (4000 ppm), whereas [NO], $[NO_2]$ and $[N_2O]$ are the concentrations of the corresponding components in the reactor effluent. The deviation of the concentrations obtained from the $m/z = 28$ MS signal and that, calculated from the equation above, was always less than ±5%. This is suggesting that CO formation, if any, was insignificantly low. In most NO-SCR experiments, only traces of NO_2 and N_2O could be detected. The conversion of methane was calculated from its concentrations in the reactant and the product mixtures. The conversion of NO to NO_2 during the NO-COX reaction was determined form the concentration of NO_2 in the effluent using the following equation:

$$\text{Conversion of NO to } NO_2\text{ (mol\%)} = \frac{[NO_2]}{[NO]^0} \times 100$$

Experiments were designed for the use of Co^{SSR},H-ZSM-5 and In,H-ZSM-5 catalysts in sequential catalyst beds in the reactor or making a single bed from the mixture of the catalysts. In these experiments, 100 mg of each catalyst sample was used to have the same amount of active metal in the reactor than at the use of 100 mg bimetallic catalysts.

2.5. Operando diffuse reflectance infrared Fourier transform spectroscopy (DRIFTS) investigations

The catalyst-bound species obtained from the NO-SCR or NO-COX reaction were studied by DRIFT spectroscopy using a Nicolet 5PC spectrometer, equipped with a COLLECTOR™ II diffuse reflectance mirror system and a flow-through DRIFT spectroscopic reactor cell (Spectra-Tech, Inc.). The same experimental conditions (temperature, reactant concentrations, and GHSV) were set at the reactor cell and the microreactor measurements. The sample cup of the cell (I.D.: 5 mm, height: 4 mm) was filled with about 20 mg of powdered sample. The spectrum of the catalyst powder was taken at every selected reaction temperatures in He-flow. This spectrum was subtracted from the corresponding spectrum of the catalyst and the reaction mixture in the cell to get characteristic difference spectrum. The concentration of the reactants and products was continuously monitored by on-line MS. The experimental set-up allowed abrupt switching between reactant mixtures NO/O_2 and CH_4/NO/O_2. The partial pressures of NO and O_2 were the same in the two gas mixtures. (The CH_4 was present on the expense of He balance gas.) After a switch the system reached a new steady state in about 4–8 min, as shown by the stabilized MS peak intensities.

3. Results

3.1. Catalyst characterization

3.1.1. H_2-TPR measurements

The H_2-TPR curves obtained for the monometallic and bimetallic catalyst samples are shown in Fig. 1. No reduction peak is observed on the curve of Co^{IE},H-ZSM-5 sample up to 1073 K (Fig. 1A). The Co^{2+} ions in ion-exchange positions of zeolites were shown to become reduced in the 973–1173 K temperature range [29–33]. Therefore, the cobalt in the Co^{IE},H-ZSM-5 sample must be lattice cation in the ion-exchange positions of the ZSM-5 zeolite. A single reduction peak appears in the H_2-TPR curves of In,H-ZSM-5 and In,Co^{IE},H-ZSM-5 samples at a temperature of about 573 K (Fig. 1A). The H_2 consumption corresponds to a 2e reduction of the indium (Table 2). Earlier reports confirmed that the RSSIE generates In^+ cations that are oxidized by O_2 to oxocations $[InO]^+$ [34–36]. The results suggest that the initial In^+ state was recovered in the H_2-TPR experiments. The presence of cobalt did not affect the reduction of the $[InO]^+$ oxocations (Fig. 1A).

A characteristic peak was obtained in the 623–673 K temperature range for the Co,H- and the Co,In,H-ZSM-5 catalysts, containing cobalt that was introduced by the SSR method (Fig. 1B). Similar H_2-TPR peak was obtained for the reduction of cobalt oxides on the outer surface of zeolite crystallites [29–33]. The calculated H/Co atomic ratio for the full reduction of CoO and Co_3O_4 ($CoO{\cdot}Co_2O_3$) is 2.0 and 2.66, respectively. Considering these values the Co^{SSR},H-ZSM-5 sample must contain both type of oxides, whereas the In,Co^{SSR},H-ZSM-5 and Co^{SSR},In,H-ZSM-5 samples contain predominantly CoO and Co_3O_4, respectively (Table 2). The H_2-TPR peak at about 573 K is similar to that found for the monometallic In,H-zeolite catalyst suggesting that the presence of Co-oxide does not influence the reduction of the $[InO]^+$ oxocations (Fig. 1B).

3.1.2. XPS results

The Co $2p_{3/2}$ and In $3d_{5/2}$ binding energies (BE) and the assignment of the corresponding species in the monometallic and bimetallic samples are given in Table 3. The BE of ~445.5 eV was assigned to the In $3d_{5/2}$ level of species $[InO]^+$ [37]. The In $3d_{5/2}$ lines are nearly the same for all In-containing samples indicating that the preparations contain similar In species and the chemical state of this species is not influenced by the presence cobalt in the catalyst. In contrast, different Co species were identified in the Co^{IE},H-ZSM-5 and Co^{SSR},H-ZSM-5 samples. Based on the BE of Co $2p_{3/2}$ level, the IE sample contains Co^{2+} ions in ion-exchange positions, whereas the SSR sample contains Co-oxide (CoO and/or Co_3O_4) as dominant species [38]. The corresponding Co $2p_{3/2}$ lines appeared in the XPS spectra also of the bimetallic catalysts. The XPS results support the conclusions of the H_2-TPR examination.

Table 2
Results of H_2-TPR experiments.

Catalyst sample	Hydrogen consumption	
	H/In	H/Co
In,H-ZSM-5	1.97	–
In,Co^{IE},H-ZSM-5	2.02	–[b]
Co^{IE},H-ZSM-5	–	–[b]
Co^{SSR},H-ZSM-5	–	2.34
In,Co^{SSR},H-ZSM-5	(2.00)[a]	2.12
Co^{SSR},In,H-ZSM-5	(2.00)[a]	2.64

[a] Assumed to calculate H/Co atomic ratio.
[b] No reduction peak was observed up to 1073 K.

3.2. Catalytic results

The H_2-TPR and the XPS measurements confirmed that the applied different methods of cobalt introduction resulted in distinctly different active cobalt sites. The monometallic catalyst, containing cationic cobalt in ion-exchange position induces NO-SCR reaction (Fig. 2A). On the contrary, in agreement with earlier results [31,39–41], the Co-oxide clusters promote the NO-COX reaction but not the NO-SCR even in the presence of methane. Nitrogen was formed only at reaction temperature over 700 K (Fig. 2B). The In,H-ZSM-5 catalyst, shown to contain $[InO]^+$ cations, selectively converted NO to N_2 (Fig. 2C, Table 3).

The conversion over the bimetallic catalysts is shown in Fig. 3. The activity of the In,Co^{IE},H-ZSM-5 catalyst (Fig. 3A) is very similar to that of the In,H-ZSM-5 (Fig. 2C), suggesting negligible interplay between the two types of active sites, i.e., between the Co^{2+} and $[InO]^+$ centers. The rate of NO conversion is similar over In,H-, In,Co^{IE},H-, and In,Co^{SSR},H-ZSM-5 catalysts in the low temperature range (up to about 700 K), whereas it is significantly higher over the In,Co^{SSR},H-ZSM-5 catalyst than on the mentioned other catalysts in the high temperature range (over about 700 K) (cf. Fig. 3B and Fig. 2C). Important to notice that in contrast to the Co^{SSR},H-ZSM-5 catalyst, which converted NO selectively to NO_2, the In,Co^{SSR},H-ZSM-5 catalyst had 100% N_2 selectivity (cf. Fig. 3B and Fig. 2B). Interestingly, the NO-SCR activity of the bimetallic samples, especially in the low temperature range (<700 K), depended on the order of metal introduction. If In was introduced first (RSSIE) and Co second (SSR) the catalyst was more active than the one prepared using the reverse order of metal introduction (cf. Fig. 3C and B).

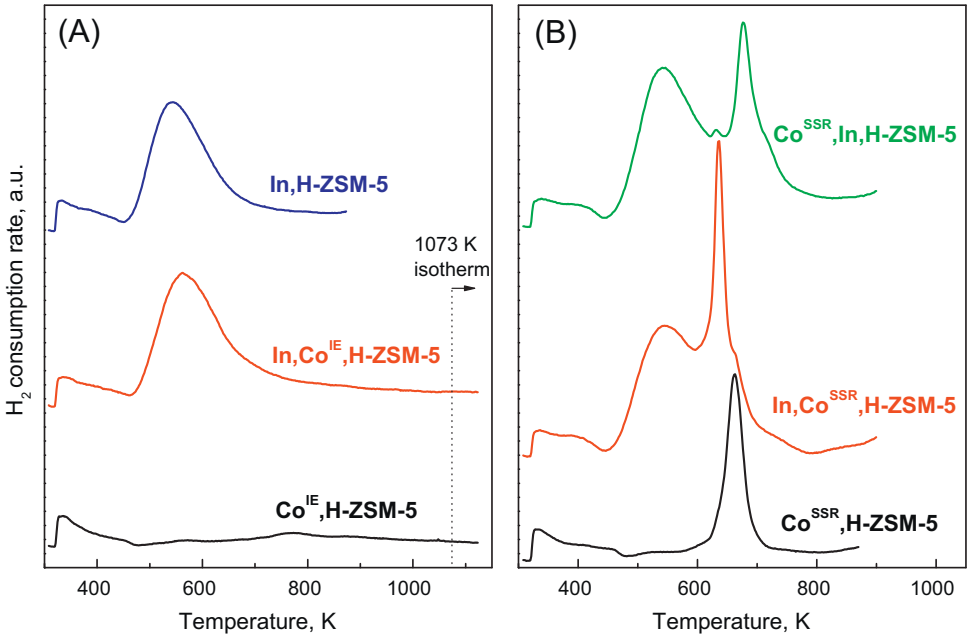

Fig. 1. Results of the temperature-programmed H_2 reduction (H_2-TPR) experiments. Catalyst samples were pretreated in O_2 flow at 773 K for 1 h before the H_2-TPR experiment then purged with N_2 at 773 K and cooled to room temperature. Reduction was initiated by switching the N_2 flow to a 10% H_2/N_2 flow and ramping the temperature at a rate of 10 K min^{-1} up to 1073 K.

Table 3
Results of the XPS experiments.

Catalyst sample	Co $2p_{3/2}$[a]	Assignment[b]	In $3d_{5/2}$[a]	Assignment[c]
In,H-ZSM-5	–	–	445.5	$[InO]^+$
Co^{IE},H-ZSM-5	782.1 787.8[d]	Co^{2+}	–	–
Co^{SSR},H-ZSM-5	780.0 787.0[d]	Co-oxide	–	–
In,Co^{IE},H-ZSM-5	782.0 787.4[d]	Co^{2+}	445.5	$[InO]^+$
In,Co^{SSR},H-ZSM-5	779.8 787.2[d]	Co-oxide	445.6	$[InO]^+$
Co^{SSR},In,H-ZSM-5	779.2 786.7[d]	Co-oxide	445.8	$[InO]^+$

[a] Binding energy values, eV.
[b] See Ref. [38] and references cited therein.
[c] See Ref. [37] and references cited therein.
[d] "Shake up" line.

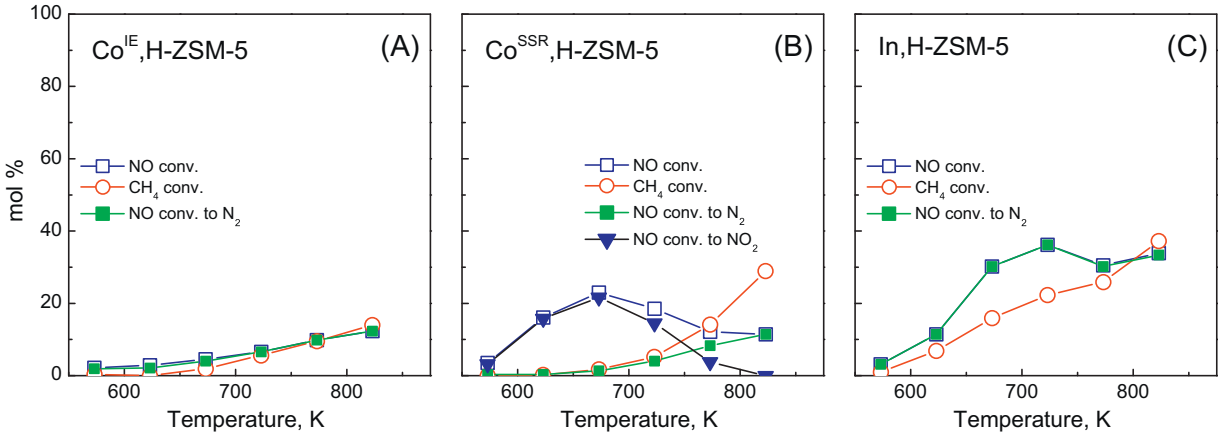

Fig. 2. The conversion of NO and CH_4 in the NO-SCR reaction over the monometallic catalysts. The reactant flow was 4000 ppm NO/4000 ppm CH_4/2% O_2/He gas mixture, the GHSV was 30 000 h^{-1}. Before reaction catalysts were treated *in situ* in 10% O_2/He flow at 773 K for 1 h then purged with He at the same temperature.

On latter catalyst small amount of NO_2 was also formed at temperatures >700 K, although the N_2 selectivity was still high (>95%) (Fig. 3C).

Above results clearly shows the importance of the interplay between the Co-oxide clusters and the $[InO]^+$ sites. The co-operation of the two kinds of sites is possible also from a certain distance. First separated but neighboring catalyst beds were made in the reactor tube from Co^{SSR},H-ZSM-5 catalyst and In,H-ZSM-5 catalyst. The NO/CH_4/O_2 reactant mixture passed first through the catalyst bed of Co^{SSR},H-ZSM-5 particles then through the bed from In,H-ZSM-5 catalyst (Fig. 4A). A notable difference of the catalytic behavior of this double-bed system from the single-bed system containing In,H-ZSM-5 catalyst is that the former one shows significantly higher NO conversion below about 700 K (cf. Fig. 4A and Fig. 2C). In another experiment, the mixture of the two catalysts was used (Fig. 4B). The catalytic behavior of this catalyst was similar to that of the corresponding bimetallic catalyst (Fig. 3C), i.e., high NO conversion was obtained in the entire applied temperature range (Fig. 4B). The selectivity of NO conversion to N_2 was high for both the double-bed and the mixed catalytic systems; nevertheless some NO_2 also appeared in the reactor effluent especially at higher reaction temperatures (Fig. 4). These results suggest that the two types of active sites—representing two catalytic functions—are separable, but the interplay between them is more effective if they are relatively close to each other.

The methane is selectively consumed in the NO-SCR if its molar conversion is half of the NO conversion to N_2 (Eq. (1)).

$$CH_4 + O_2 + 2NO \rightarrow CO_2 + 2H_2O + N_2 \quad (1)$$

Higher conversion indicates that methane reacted also directly with O_2 ($CH_4 + 2O_2 \rightarrow CO_2 + 2H_2O$). The reaction, referred to as methane combustion, usually occurs at temperatures above 700 K (Figs. 2–4).

The thermodynamics allows high conversion of NO and O_2 to NO_2 below about 700 K (Fig. 5). Without catalyst (with quartz wool in the reactor), however, the NO conversion remained very low (1–2%) (Fig. 5A). Many results suggest that NO_2 is an important intermediate of the NO-SCR reaction. Therefore, the NO-COX activity of the catalysts was measured in the absence of methane. The conversion is shown as a function of reaction temperature (Fig. 5). In line with expectations [31,39,40] the Co^{SSR},H-ZSM-5 sample was very active (Fig. 5A). The NO_2 formation is kinetically controlled at temperatures below about 650 K, whereas thermodynamic control is effective above about 650 K [25,31,40,41]. As compared to Co^{SSR},H-ZSM-5 the pure H-form of the zeolite (H-ZSM-5) shows significantly lower but still considerable NO-COX activity (Fig. 5A), showing that the reaction proceeds also on Brønsted acid sites. Latter finding is in correspondence with earlier results [7,8,25]. Practically the same conversion curve was observed for the Co^{IE},H-ZSM-5 than for the H-ZSM-5 catalyst (Fig. 5A) indicating that the Co^{2+} cations in ion-exchange positions do not contribute to the NO-COX activity. Similar results were presented for different Co-zeolite

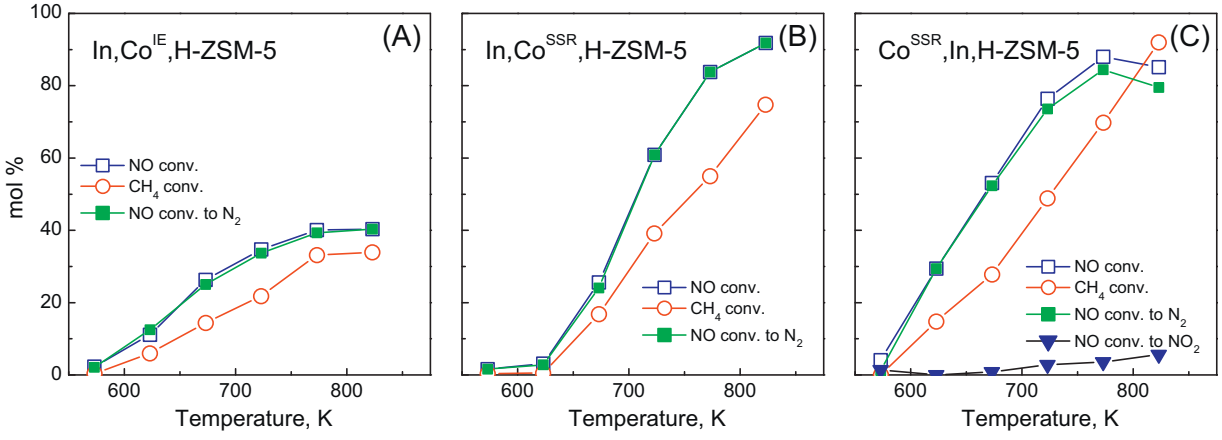

Fig. 3. The conversion of NO and CH_4 in the NO-SCR reaction over the bimetallic catalysts. For experimental details see the legend of Fig. 2.

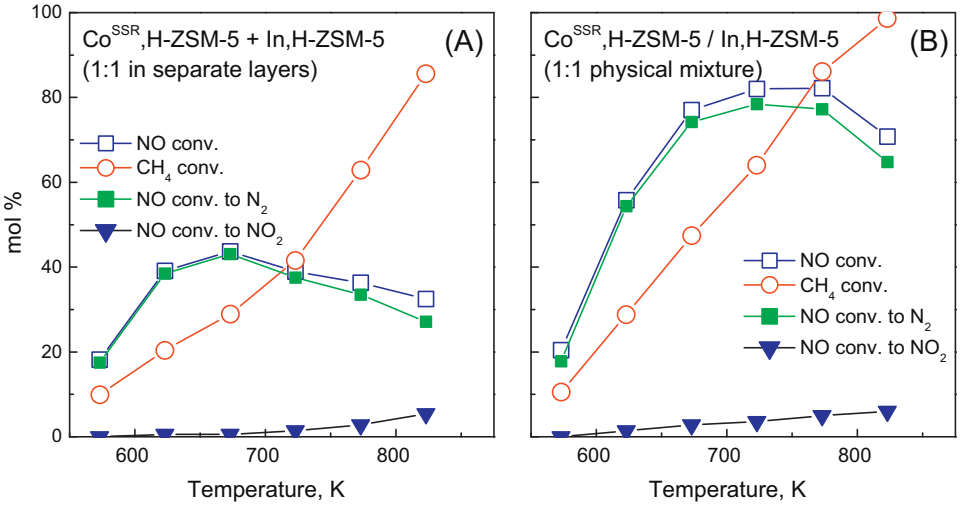

Fig. 4. The conversion of NO and CH_4 in the NO-SCR reaction over the Co^{SSR},H-ZSM-5/In,H-ZSM-5 double catalyst system. Equal amounts of catalysts were placed into the tube reactor as (A) neighboring catalyst beds and (B) as catalyst mixture. The GHSV was 15 000 h^{-1}. For other experimental details see the legend of Fig. 2.

catalysts, which results substantiated that Co ions exhibit activity in the CH_4/NO-SCR, whereas protons and oxide-like Co species are active in the NO-COX reaction [42]. Both the In,H-ZSM-5 and In,Co^{IE},H-ZSM-5 samples show lower NO-COX activity than the H-ZSM-5 (Fig. 5B). These catalysts contain fewer active Brønsted acid sites than the H-form zeolite because more than 30% of the framework charge is balanced by metal cations. Neither the Co^{2+} nor the $[InO]^+$ lattice cations seem to be active in the NO-COX reaction. This conclusion is in accordance with those of Kikuchi et al. [7,8], who showed that the NO-COX and CH_4/NO-SCR reactions proceed on Brønsted acid sites and cationic indium sites, respectively. The bimetallic In,Co^{SSR},H-ZSM-5 and Co^{SSR},In,H-ZSM-5 catalysts have NO-COX activity as high as that of the Co^{SSR},H-ZSM-5 catalyst (cf. Fig. 5A and B) further confirming that the rate of the NO-COX reaction is significantly increased by the presence of Co-oxide clusters.

3.3. Operando DRIFTS-MS examinations

3.3.1. Species from adsorption of NO/O_2 mixture

Difference DRIFT spectra of the catalysts in contact with NO/O_2 flow at 573 K are shown in Figs. 6 and 7. All the bands became weaker if temperature was raised and increased in intensity if the temperature was lowered (not shown). All the adsorbed species were removed by a He flush at 773 K. These results show that the adsorption was relatively weak and reversible.

The spectrum of the adsorbed species on the pure H-form shows bands at 2127 and 1640 cm^{-1} stemming from ν_{NO} and δ_{H_2O} vibrations of zeolite-bound nitrosonium ions (NO^+) and water, respectively [43]. The formation of the adsorbed species was accompanied by the consumption of Brønsted acidic hydroxyl groups, as indicated by the negative ν_{OH}-band at 3600 cm^{-1} (Fig. 6A). These spectral features were interpreted by the overall process of Eq. (2) [43]:

$$2H^+Z^- + NO + NO_2 \rightleftarrows 2NO^+Z^- + H_2O \quad (2)$$

where Z^- represents a segment of the zeolite framework carrying one negative charge. The zeolite, partially ion-exchanged with indium and/or cobalt (Table 1) contains also protons as cations. Therefore, this process takes place on each sample as shown by the corresponding spectral features. We note here that the intensity loss of the ν_{OH} band is due to the replacement of the protons by

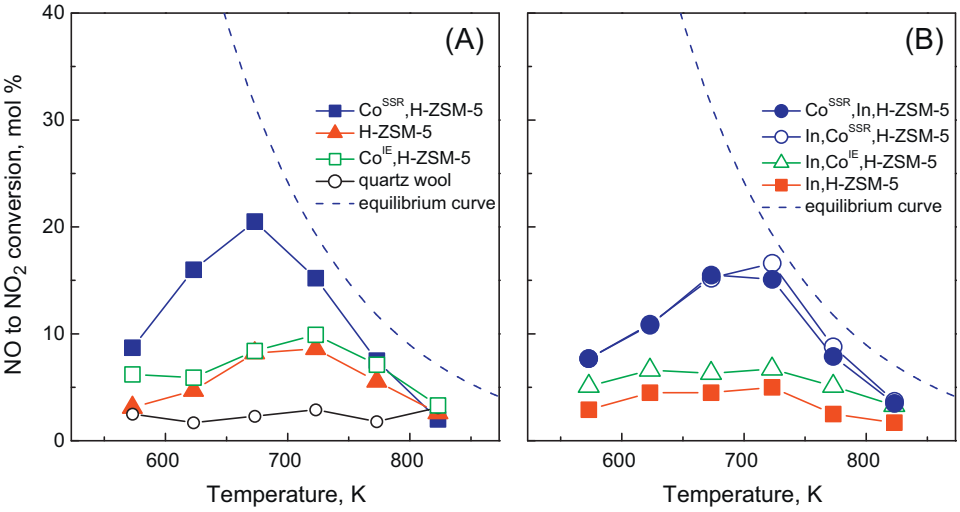

Fig. 5. The conversion of NO to NO_2 by O_2. The reactant was 4000 ppm NO/2% O_2/He gas mixture, the GHSV was 30 000 h^{-1}. The dashed curve shows the equilibrium concentration of NO_2.

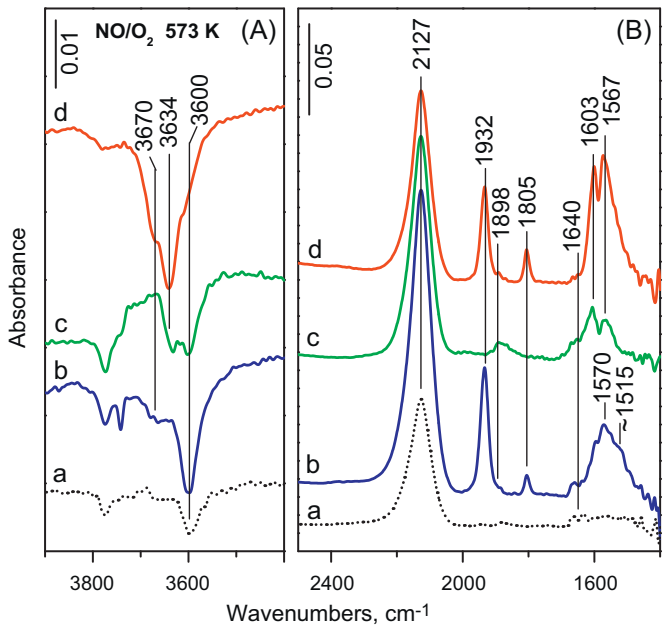

Fig. 6. Difference DRIFT spectra of the catalyst (a) H-ZSM-5, (b) Co^{IE},H-ZSM-5, (c) In,H-ZSM-5 and (d) Co^{IE},In,H-ZSM-5 in contact with a continuous flow of 4000 ppm NO/2% O_2/He gas mixture at GHSV 30 000 h^{-1} and 573 K. (A) The ν_{OH} region and (B) the species obtained from adsorption.

NO^+ and to some extent due to the H-bonding interaction of water with the hydroxyl groups inducing red shift of the ν_{OH} band.

Additional species were formed on the Co^{IE},H-ZSM-5 sample giving characteristic band at 1570 cm^{-1} with a shoulder at ~1515 cm^{-1}, at 1932, 1898, and 1805 cm^{-1} (Fig. 6B, spectrum b), and a new negative ν_{OH} band at ~3670 cm^{-1} (Fig. 6A, spectrum b). The hydroxyl groups giving band at 3670 cm^{-1} were generated from water on Co^{2+} sites ($Co^{2+}Z_2^- + H_2O \rightleftarrows [Co\text{-}OH]^+Z^- + H^+Z^-$) [29,44,45]. The negative ν_{OH} band therefore indirectly indicates the involvement of the cationic Co sites in the formation of surface

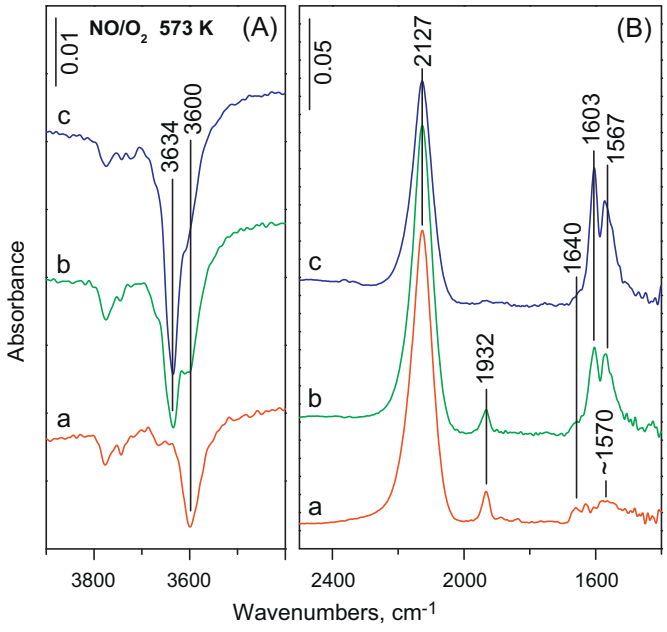

Fig. 7. Difference DRIFT spectra of the catalyst (a) Co^{SSR}-ZSM-5, (b) In,Co^{SSR},H-ZSM-5 and (c) Co^{SSR},In,H-ZSM-5 in contact with a continuous flow of 4000 ppm NO/2% O_2/He gas mixture at GHSV 30 000 h^{-1} and 573 K. (A) The ν_{OH} region and (B) the species obtained from adsorption.

species giving positive absorption bands. Earlier studies attributed the bands in the 1500–1650 cm^{-1} range to the formation of NO_x^- species, particularly to differently bound nitrate, NO_3^- species [28,46]. The formation of NO_3^- species from the adsorption of NO/O_2 mixture is generally accompanied by the formation of NO^+ species [28,44,46–48]. In a recent study [44] we suggested that the NO_3^- and NO^+ surface species were formed on $[Co\text{-}OH]^+$ sites according to Eq. (3):

$$[Co\text{-}OH]^+Z^- + H^+Z^- + 2NO_2 \rightleftarrows [Co\text{-}NO_3]^+Z^- + [NO]^+Z^- + H_2O \quad (3)$$

The process takes place simultaneously with that according to Eq. (2) as shown by the negative ν_{OH} band at 3600 cm^{-1}. The absorption bands in the 1750–1950 cm^{-1} range are usually attributed to different nitrosyls and dinitrosyls of ionic cobalt in zeolites [49]. The pair of bands at 1805 and 1898 cm^{-1} come from the absorptions corresponding to the symmetric and asymmetric stretching vibrations of Co^{2+}-dinitrosyl species [28,50–52]. The assignment of the band at 1932 cm^{-1} (Fig. 6B, spectrum b) is less straightforward. It was attributed either to Co^{2+}-mononitrosyl [50,51] or to Co^{3+}-mononitrosyl in Co-ZSM-5 [28,52]. Recent works accepted this latter assignment emphasizing, however, that the species must carry an oxygen ligand (CoO^+) that lowers the charge on the cobalt [53,54]. It was argued that it is highly improbable that bare ions could neutralize three distant negative charges of the zeolite having high framework Si to Al ratio (>15). The oxygen-carrying Co^{3+} was expected to get reduced at lower temperature than the Co^{2+} ions [29–33]. The H_2-TPR results, however, did not confirm the presence of any Co^{3+} species in our Co^{IE},H-ZSM-5 sample as no reduction peak could be observed up to 1073 K (Fig. 1A). Therefore, it seems likely that this sample contains mainly hard-to-reduce Co^{2+} species and the corresponding band can be assigned to Co^{2+}-mononitrosyl [50,51]. Since the mononitrosyl band dominates it is assumed that Co^{2+} is mainly in the form of $[Co\text{-}OH]^+$, which can accommodate only one nitrosyl ligand because its coordination sphere is already partially saturated by a hydroxyl group [55].

The spectrum of the In,H-ZSM-5 presents a new pair of bands at 1603 and 1567 cm^{-1} (Fig. 6B, spectrum c), which can be attributed to NO_3^- species [23,56], most probably to bridging bidentate nitrato and chelating bidentate nitrate species, respectively [49]. The formation of surface nitrate species is accompanied by the appearance of a negative ν_{OH} band at 3634 cm^{-1} (Fig. 6A, spectrum c). This band, which developed only in the spectrum of the In-containing samples, stems most probably from In-related OH-groups [23]. These hydroxyl groups are similar to those obtained via heterolytic water dissociation on Co^{2+} sites (see above) [44,45]. The occurrence of similar reaction between H_2O and $[InO]^+$ cations, which were found to be also strong Lewis acid centers [34,35], cannot be excluded. Recent results, however, substantiated the formation and stabilization of protonated InO^+ species, such as $[In_4(OH)_4]^{8+}$ units, in the β-cages of zeolite Y [57]. In zeolite In,H-ZSM-5 catalyst the occurrence of monomeric $[InOH]^{2+}$ species seems to be more likely, because of the low concentration of the balancing negative framework charge. Note that the reduction of both the $[InO]^+$ and the $[InOH]^{2+}$ species to In^+ requires the oxidation of two H-atoms (Table 2.). The annihilation of the In-related hydroxyl groups is concomitant with the formation of surface NO_3^-, suggesting that the $[InO]^+/[InOH]^{2+}$ species participate in the nitrate-forming reaction. In a previous communication we have shown that the NO_3^- species are always formed together with NO^+ on In-zeolites [23]. The process was described by Eq. (4).

$$[InOH]^{2+}Z_2^- + NO + NO_2 \rightleftarrows [NO]^+Z^- + In^+NO_3^- + H^+Z^- \quad (4)$$

This process takes place parallel to that on Brønsted acid sites according to Eq. (2) as indicated by the appearance of the negative ν_{OH} bands at 3634 cm^{-1} and also at 3600 cm^{-1} (Fig. 6A, spectrum c).

All the reactions according to Eqs. (2)–(4) occur simultaneously on the bimetallic Co^{IE},In,H-ZSM-5 sample as indicated by the corresponding negative ν_{OH} bands (Fig. 6A, spectrum d) and other absorption bands characteristic of surface NO^+ (2127 cm^{-1}), Co^{2+}-nitrosyl (1932, 1898 and 1805 cm^{-1}), and NO_3^- (1603 and 1567 cm^{-1}) species (Fig. 6B, spectrum d). Latter two bands appear with higher intensity and broadened at the low frequency side compared to the corresponding bands obtained for the In,H-ZSM-5 catalyst (cf. Fig. 6B, spectra c and d) suggesting that the bands of the In-bound nitrates (Fig. 6B, spectrum c) are superimposed on the bands of Co-bound nitrates (Fig. 6B, spectrum b).

When Co is present predominantly in the form of Co-oxide clusters (shown by H_2-TPR and XPS) and only negligible amount belongs to the zeolite lattice, as in the Co^{SSR},H-ZSM-5 catalyst, nitrosyl bands and nitrate bands are hardly discernible (Fig. 7B, spectrum a). These results are in accordance with the observation that nitrosyls and nitrate species can form on ionic cobalt, whereas such surface species are not formed on Co-oxide clusters [29,53]. Since neither the NO adsorption nor the process of Eq. (3) proceeds on Co-oxide clusters, the spectrum obtained on the Co^{SSR},H-ZSM-5 catalyst in contact with NO/O_2 mixture closely resembles that obtained for the H-ZSM-5 (cf. Figs. 6 and 7, spectrum a) substantiating that only the process according to Eq. (2) prevails on this sample. Similarly, the spectra obtained for the bimetallic In,Co^{SSR},H-ZSM-5 and Co^{SSR},In,H-ZSM-5 correspond to that obtained for the monometallic In,H-ZSM-5 sample (cf. Fig. 7, spectra b and c, and Fig. 6, spectrum c) indicating that processes of NO oxidation and formation of NO^+ and NO_3^- (Eqs. (2) and (4)) proceed on these samples. However, the NO_3^- bands (1603 and 1567 cm^{-1}) and the negative ν_{OH} band (3634 cm^{-1}) of the two catalysts show substantial intensity difference. The surface concentration of the NO_3^- species is higher on the bimetallic catalysts and is the highest on the Co^{SSR},In,H-ZSM-5 catalyst (Fig. 7B, cf. spectra b and c). Note that this sample contains Co-oxide clusters mainly in the form of Co_3O_4 (Table 2). Results suggest that the rate of the process according to Eq. (4) is the highest on the Co-oxide-containing bimetallic catalyst, having the highest NO-COX activity.

3.3.2. *The reaction of surface-bound NO_x and methane*

The steady state of the catalytic system, comprising of catalyst and reactant NO/O_2/He flow, was disturbed by suddenly changing the gas flow to a flow of $CH_4/NO/O_2$/He, while the partial pressures of NO and O_2 were kept unchanged. The transient change of the effluent composition, monitored by MS, gave a pattern for all the studied catalysts, similar to that shown in Fig. 9D. The adsorbed species approached new, lower steady state concentrations (Figs. 8 and 9, bottom spectra). The steady state NO to N_2 conversions are in good agreement with those obtained in the corresponding catalytic microreactor experiments (Figs. 2 and 3).

The Co^{IE},H-ZSM-5 and Co^{SSR},H-ZSM-5 catalysts showed somewhat different responses to methane (Fig. 8). The NO^+ (2127 cm^{-1}), Co-mononitrosyl (1932 cm^{-1}), and NO_3^- (1570 and ~1515 cm^{-1}) bands of the former sample slightly decreased, whereas those of the latter sample remained practically unchanged. In line with the relatively small NO-SCR activity of the Co^{IE},H-ZSM-5 catalyst small amounts of NO-SCR products, such as CO_2 (bands at 2362 and 2332 cm^{-1} in the IR spectra and also detected by MS) and N_2 (detected by MS) were discernible (Fig. 2A). Earlier studies substantiated that surface nitrates formed on the Co sites are reactive with methane and can initiate the NO-SCR reaction [28,44,46]. It was however excluded that different cobalt nitrosyls were active intermediates of the NO-SCR reaction [28,46]. It was also shown that the Co-mononitrosyl giving the band at 1932 cm^{-1} is particularly sensitive to water [28]. The intensity drop of this band (Fig. 8A) is therefore attributed to the displacement of the nitrosyl species by water formed during the SCR reaction. This is also supported by the fact that the nitrosyl band did not lose intensity in absence of SCR activity (Fig. 8B).

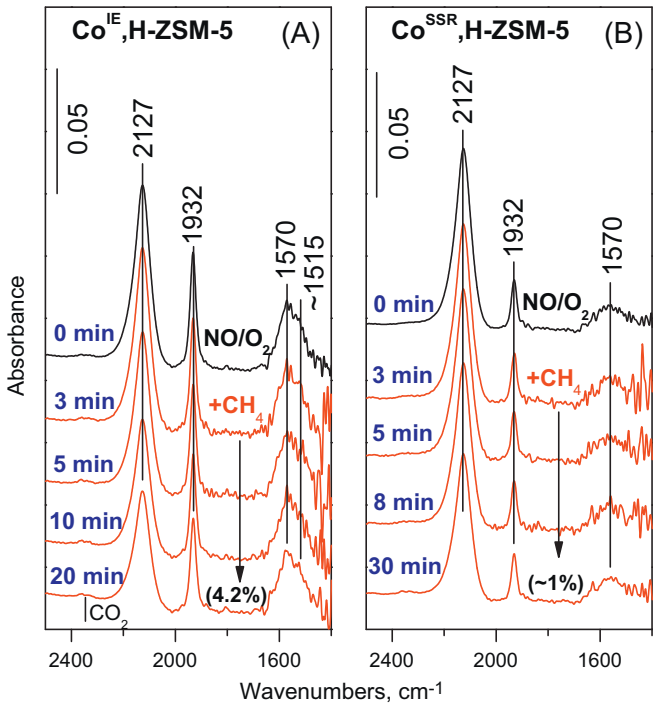

Fig. 8. Operando DRIFTS examination of the transient response of the catalyst on the change of the reactant composition. Catalysts (A) Co^{IE},H-ZSM-5 and (B) Co^{SSR},H-ZSM-5 were contacted with a flow of 4000 ppm NO/2% O_2/He at GHSV 30 000 h^{-1} and 623 K. The first spectrum was recorded after the steady state was established (uppermost spectrum), then the flow was abruptly changed to a similar flow of 4000 ppm NO/4000 ppm CH_4/2% O_2/He (indicated as $+CH_4$). Spectra were recorded after the given time on the stream. The spectrum of the catalyst in He at 623 K was subtracted from each spectrum and the difference spectrum is shown. The numbers in parenthesis give the percent conversions of NO to N_2 in the steady state.

The NO_3^- species formed on $[InO]^+$ sites are much more reactive with methane than those formed on Co^{2+} sites. The intensity of the 1603 and 1567 cm^{-1} bands decreases at a higher rate for the more active In-containing catalysts (cf. Fig. 8A and Fig. 9A–C). The reactivity of the nitrate is reflected by the NO-SCR activity of the catalyst (cf. Fig. 2A and Fig. 3A–C). The consumption of surface NO_3^- species and the formation of N_2 and CO_2 take place simultaneously and occur when CH_4 appears in the feed (Fig. 9C and D). The initial overshoot of the N_2 and CO_2 concentrations of the effluent comes from the higher initial surface concentration of the nitrate than in the new steady state being approached.

The consumption of NO_3^- species in the CH_4/NO-SCR reaction is accompanied by the consumption of NO^+ species as it is clearly shown by the concomitant intensity drop of the corresponding bands (Fig. 9A–C). In a former study [23] we have shown that the NO^+ alone, cannot react with methane. Conversely, the NO^+, formed together with NO_3^- (Eq. (4)) was also consumed together in the NO-SCR reaction [23]. No doubt, however, that the surface concentration of NO^+ must have been decreased also, because the product water of the NO-SCR reaction shifted the equilibrium of Eq. (2).

The concentration of mononitrosyls on the catalyst surface did not show any correlation with the NO-SCR activity. For instance, the presence of reacting methane decreases the mononitrosyl concentration over the In,Co^{IE},H-ZSM-5 catalyst. However, the catalyst shows the same catalytic activity as the In,H-ZSM-5 catalyst, not presenting nitrosyl–forming ability (cf. Fig. 2C and Fig. 3A). Furthermore, the catalysts, not carrying Co-mononitrosyl at all, show higher NO-SCR activity than those, able to generate surface nitrosyl

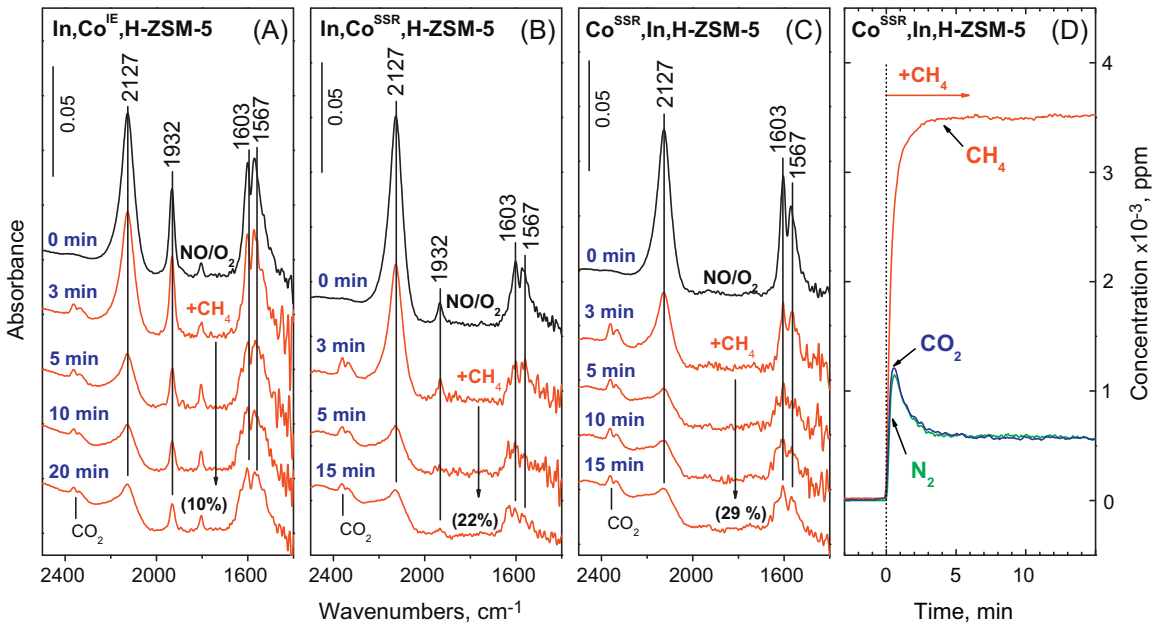

Fig. 9. Operando DRIFTS examination of the transient response of the catalyst on the change of the reactant composition. Catalysts (A) In,Co^{IE},H-ZSM-5, (B) In,Co^{SSR},H-ZSM-5 and (C) Co^{SSR},In,H-ZSM-5 were examined in experiments described in the legend of Fig. 8. Part (D) gives the CH_4, N_2 and CO_2 concentrations of the effluent from experiment (C) as a function of time from the moment of switching the NO/O_2/He flow to a flow of $CH_4/NO/O_2$/He.

(Fig. 3B and C and Fig. 9B and C). The elimination of Co-mononitrosyl species during NO-SCR reaction can be again attributed to their displacement by product water [28], which is more pronounced at higher water concentrations corresponding to the higher rates of the NO-SCR reaction. Results also show that, in agreement with earlier observations [28], the sensitivity of mononitrosyl species (band at 1932 cm^{-1}) to water is significantly higher than that of dinitrosyl species giving the characteristic bands at 1898 and 1805 cm^{-1} (Fig. 9A).

Thus, in agreement with earlier findings [28,46], we exclude that mononitrosyl species could play any role in the NO-SCR mechanism.

4. Discussion

4.1. The Co and In species in the catalysts

The conventional ion-exchange (IE) of H-zeolite with cobalt-containing solution and the thermally induced transformation of the solid H-zeolite/cobalt acetate mixture resulted in different Co-catalysts. The ion-exchanged sample contains Co-ions, identified as Co^{2+} and/or $[Co\text{-}OH]^+$ cations, occupying ion-exchange positions within the zeolite. In contrast, the solid state reaction (SSR) resulted in the formation of Co-oxide clusters, mainly Co_3O_4 clusters (Table 2) on the outer surface of the H-zeolite crystallites. The ion-exchanged Co,H-form zeolite remained virtually the same upon In-introduction by RSSIE. Also, the solid state reaction generated similar cobalt oxide clusters on In,H-zeolite than on the H-zeolite. However, the composition of Co-oxide clusters depended on the introduction sequence of the metal components. When indium was introduced prior to the cobalt (Co^{SSR},In,H-ZSM-5) the dominant cobalt species was Co_3O_4, whereas the reverse order of introduction resulted in mainly CoO clusters (In,Co^{SSR},H-ZSM-5) (Table 2). The lower average oxidation state of Co in the latter sample is the consequence of the reductive treatment applied to introduce the In as a second metal by the RSSIE method.

In agreement with expectations [34–36] all the In-catalysts contained $[InO]^+/[InOH]^{2+}$ cations in ion-exchange positions.

4.2. The promoting effect of Co

The promoting effect of Co on the NO-SCR reaction can be clearly attributed to the activity of the cobalt species in the NO-COX reaction. In agreement with earlier results Co-ions in exchange position show activity in the N_2 forming CH_4/NO-SCR reaction (Fig. 2A) [3,20,21,29,32,42,44,45] but do not contribute to the NO-COX activity of the catalyst (Fig. 5A) [3,58]. Conversely, as it was reported earlier [31,39–41], the Co-oxide clusters catalyze the NO_2-generating NO-COX reaction (Figs. 2B and 5A), but not the N_2 forming catalytic methane oxidation. It should be noted, however, that over about 700 K nitrogen is formed (Fig. 2B), in a kind of catalytic process over cobalt and/or acidic sites [59]. The higher activity of the bimetallic samples (Fig. 3) clearly indicate that the NO-SCR activity of In,H-ZSM-5 is enhanced by the Co-oxide clusters, whereas exchange Co-ions practically do not have any promoting effect. Studying a similar catalytic system Kubacka et al. [21] attributed the enhanced NO-SCR activity to the synergetic effect of Co(II) species (as exchange cation Co^{2+} or Co^{2+} in Co(II)-oxide) on the $[InO]^+$ sites, whereas the Co-oxide aggregate, particularly the Co_3O_4 was believed to promote the undesired methane combustion [4,21,32]. Indeed, the Co-oxide clusters induce also methane combustion but it becomes excessive over about 700 K (Fig. 3B and C). The here presented results clearly show that the Co-oxide clusters (especially the Co_3O_4) catalyze the NO-COX reaction and thereby promote the NO-SCR reaction, i.e., it sets forth the same promoting mechanism as the formerly suggested vide variety of promoters [10,12,14,15,17,19,22].

4.3. The NO_2 as NO-SCR intermediate

In agreement with other studies [10,12,14,15,17,19–22] our results confirm that NO_2 is important intermediate of the NO-SCR process. The NO-SCR reaction proceeds with high N_2 selectivity over In-zeolite catalysts both in the presence and the absence of cobalt oxide, but with much higher rate if cobalt oxide is present. The Brønsted acid sites were shown to have NO-COX activity (Fig. 5A) [8,25,42]. The Co-oxide clusters enhanced the NO-COX activity (Fig. 5) and thereby the NO-SCR activity (Fig. 3B and C).

This finding emphasizes that NO_2 has important role in the catalytic mechanism (cf. Fig. 3B and C and Fig. 2C). The observed high N_2 selectivity, however, suggests that the NO_2 formed in the NO-COX reaction had to be quickly consumed in the N_2-forming CH_4/NO-SCR reaction. This latter reaction uses $[InO]^+$ species as active sites [7–13].

The In-zeolite catalysts did not show activity in the reaction between CH_4 and NO but were active in the reaction between CH_4 and NO_2. This explains the importance of O_2 in the NO polluted gas and the NO-COX activity of the catalyst [8,11,17].

4.4. The NO-COX and CH_4/NO-SCR catalytic functions

Results of the present study suggest that there must be two catalytic functions, having NO-COX and CH_4/NO-SCR activity, in an effective NO-SCR catalyst. Catalysts containing active sites for the NO-COX reaction only, such as Co-oxide clusters and/or Brønsted acidic sites, do not have NO-SCR activity (Fig. 2B), whereas catalysts of low NO-COX activity have low NO-SCR activity. Concerning the NO-COX activities (Fig. 5) it is clear that Co-oxide clusters are more active than the Brønsted acid sites. The exchange cations are inactive in the NO-COX reaction. These latter species however provide the catalytic function for the N_2-forming CH_4/NO-SCR reaction. The activity of transition metal exchange cations is attributed to their ability to form active nitrates (vide infra).

The activity of Brønsted acid sites in the NO-COX reaction was shown by several studies [7,8,25,42]. The catalyst that contains Brønsted acid sites, Co^{2+} and $[Co\text{-}OH]^+$ cations has both of the necessary catalytic functions for the NO-SCR reaction (Fig. 2A). The activity of our Co^{IE},H-ZSM-5 catalyst is relatively low compared to the corresponding published results [30–32,44,45]. The low activity is attributed to the relatively low $Co^{2+}/[Co\text{-}OH]^+$ concentration of the catalyst. In contrast, the Co^{SSR},H-ZSM-5 sample containing predominantly Co-oxide clusters and only a minor amount of ionic cobalt is active exclusively in the NO-COX reaction (Fig. 2B).

The catalytic functions providing NO-COX and CH_4/NO-SCR activity were found separable. If an NO-COX catalyst is positioned in front of a CH_4/NO-SCR catalyst (Fig. 4A) the NO-SCR activity is increased in the low temperature range (<650 K), where the NO_2 formation was kinetically controlled (cf. Fig. 4A and Fig. 2B). Over about 650 K where the NO_2 concentration approaches the thermodynamic limit value [31,40,41], the NO-COX catalyst promotes the NO-SCR activity as far as thermodynamics allows. The NO_2 formed in the NO-COX reaction (on Co-oxide clusters) is rapidly removed from the system through the CH_4/NO-SCR reaction. Hindered transport of NO_2 between the sites of the two catalytic functions can determine the rate of the NO-SCR process. Using a catalyst having the catalytic functions in close proximity, the limitation raised by the rate of NO_2 transport can be removed (Fig. 4B). Similar conclusions were drawn using a CeO_2-In-ZSM-5 [24] or a Co/ZrO_2-Pd/sulfated zirconia [26,27] dual catalytic systems. In these catalytic systems, the first component was used to provide the NO-COX activity, whereas the second component served as CH_4/NO-SCR catalyst.

4.5. The cooperation of the NO-COX and the CH_4/NO-SCR reactions

The activity of the $Co^{2+}/[Co\text{-}OH]^+$ or $[InO]^+/[InOH]^{2+}$ sites in the NO-SCR reaction is clearly related to their ability to form surface nitrate species. In absence of such cationic species surface nitrate formation and NO-SCR reaction does not proceed (Figs. 6 and 7). The NO_3^- formation in the studied system can be described by the reactions of Eqs. (3) and (4) [23,44]. These reactions require both NO and/or NO_2 what means that at least a fraction of the reactant NO must be oxidized to NO_2 in order that surface nitrate should be obtained from the contact of the catalyst and the reactant gas. We showed above that the NO-COX reaction proceeds on the Brønsted acid sites and at a higher rate on the Co-oxide clusters. Thus, the Co-oxide clusters help the formation of surface nitrate over the $[InO]^+/[InOH]^{2+}$ species by more rapidly supplying NO_2 to the surface reaction of Eq. (4). This is reflected by higher steady state NO_3^- concentration on the bimetallic catalyst (Fig. 7) than on the monometallic In,H-ZSM-5 catalyst (Fig. 6). The nitrate concentration bears relation also to the concentration of the Co_3O_4 phase having high NO-COX activity (Table 2.).

In harmony with earlier conclusions [16,23,30,31,44,46] the operando DRIFTS results confirm that the nitrate formed on cationic $[InO]^+/[InOH]^{2+}$ or $Co^{2+}/[Co\text{-}OH]^+$ sites participate in the CH_4/NO-SCR reaction resulting in N_2 formation (Figs. 8 and 9). The nitrate can react with methane giving the active intermediate of the CH_4/NO-SCR reaction. This reaction was substantiated as the rate determining step of the NO-SCR process [60,61]. We could not identify the active intermediate because of its fast conversion to SCR product N_2, CO_2, and H_2O. It could be nitromethane, as it is often suggested [3,50,61]. The surface nitrate species that formed prior to the rate determining step was detectable in the steady state at 623 K where the rate of the SCR reaction was relatively low (Fig. 9). These results suggest that consumption rate of surface nitrate species is lower than the transformation rate of the substantiated nitromethane intermediate, which is in full agreement with the suggestion that methane activation is the rate determining step of the NO-SCR process.

In a recent study [23] we reported that surface NO^+ species, formed together with NO_3^- species (Eqs. (3) and (4)), also take part in the NO-SCR reaction. However, the NO^+ alone, when are formed, for instance on Brønsted acid sites according to Eq. (2), cannot initiate the CH_4/NO-SCR reaction (Fig. 8B). When formed together with NO_3^-, the NO^+ and NO_3^- were quickly and parallel consumed (Fig. 9). These results suggest that the NO^+ reacts with the intermediate generated in the reaction of methane and the zeolite-bound indium nitrate or with the transformation product(s) of this intermediate. The formal oxidation state of nitrogen in the NO^+ and in the intermediate are 3+ and 3−, respectively, satisfying the criterion of N_2 formation in the reaction of two nitrogen-containing species [23,and references cited therein]. Following this N_2-forming reaction the charges within the zeolite lattice remain balanced if In^+ species take over the role of the consumed NO^+ species. Conversely, since In^+ species are formed from charge neutral $InNO_3$ species, NO^+ species must be consumed in the reaction in order to keep the charge balance, which is in accordance with the observations. The closure of the catalytic cycle and the maintenance of the activity require that In^+ species should be oxidized to $[InO]^+$, which was shown to proceed easily even below 373 K by NO or NO_2 and above about 573 K also by O_2 [23]. Under NO-SCR conditions the $[InO]^+$ sites are most probably restored by NO_2 that is the most effective oxidizing agent, which is present in the reacting system. It follows from the stoichiometry of Eq. (1) that the ratio of converted NO and CH_4 should exceed the value of two if NO participated in this additional oxidation process. Such deviation from the stoichiometry of Eq. (1) was never observed. The outlined catalytic cycle is shown by Scheme 1.

Scheme 1 clearly shows how the NO-SCR activity is connected to and depends on the NO-COX activity. Considering that the activation of methane is the rate determining step of the NO-SCR reaction, it follows form the above arguments that higher rate of NO_3^-/NO^+ formation (Eq. (4)) leads to a higher rate of the CH_4/NO-SCR reaction. Accordingly, we found that on Co-oxide clusters the reaction of NO and O_2 to NO_2 was significantly faster than on Brønsted acid sites, increasing the formation rate of NO_3^-/NO^+ pairs, thereby, the rate of methane activation and the rate of the whole NO-SCR process. It follows from the above discussion that the rate of NO_3^-/NO^+

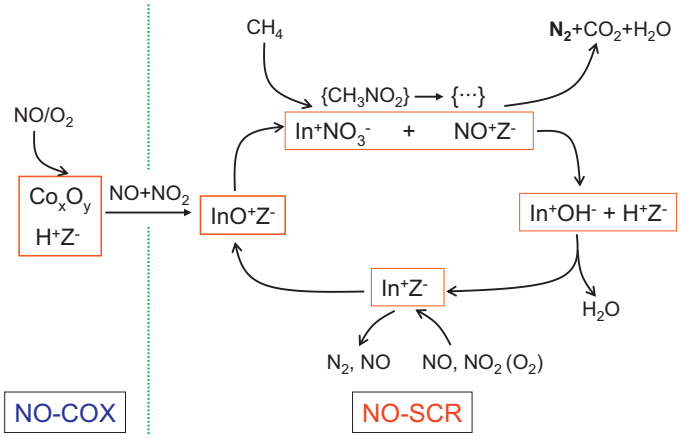

Scheme 1.

formation and thus the rate of the NO-SCR reaction is the highest over the In-zeolite catalyst if the reactant mixture contains equal amounts of NO to NO_2. Ogura et al. [11] studied the SCR reaction with different NO/NO_2 mixtures on In,H-ZSM-5 catalyst at 673 K. Indeed, the conversion reached maximum at NO/NO_2 molar ratio of 1.

The above-described connection between the NO-COX and CH_4/NO-SCR reactions infers that a proper balance between the activities of these catalytic functions is needed to have the highest NO-SCR activity and selectivity. High NO-COX activity and insufficient CH_4/NO-SCR activity of the catalyst results in the appearance of NO_2 in the product gas, decreasing the N_2 selectivity [30,31,42]. The simultaneous NO_2 and N_2 formation in the NO-SCR made some authors to think that NO_2 could not be the intermediate of the NO-SCR reaction [30,31]. The importance of the balanced activities was demonstrated by Ozkan et al. [26,27]. They tuned the catalyst system by changing the relative amount of catalyst components having NO-COX and NO-SCR activity to get minimum NO_2 yield and maximum N_2 yield. On our catalyst samples (except Co^{SSR},H-ZSM-5) the SCR reaction proceeds with a high N_2 selectivity, suggesting that the rate of the N_2-forming reaction is always high enough relative to the rate of the NO_2-forming reaction.

It follows from Scheme 1 and the above discussion that the N_2-forming CH_4/NO-SCR reaction should be distinguished from the overall NO-SCR process, which involves both the CH_4/NO-SCR and NO-COX reactions. The CH_4/NO-SCR reaction can be selective for N_2 formation, whereas the N_2 selectivity of the overall NO-SCR reaction may be lower if for any reason the NO_2 formed in the NO-COX reaction is not fully consumed in the coupled CH_4/NO-SCR reaction.

5. Conclusions

Present study confirmed that the selective catalytic reduction of NO by methane requires two catalytic functions: one for initiating the oxidation of NO to NO_2 (NO-COX) and another for the N_2-forming reaction (CH_4/NO-SCR). The NO-COX reaction proceeds over the Brønsted acid sites and, if present, also over Co-oxide clusters. The Co-oxides, especially the Co_3O_4 are much more active than the acidic hydroxyl groups. The N_2-forming CH_4/NO-SCR reaction is catalyzed by Co^{2+}/$[Co\text{-}OH]^+$ or $[InO]^+$/$[InOH]^{2+}$ ions. In the NO-COX reaction NO_2 is formed that is needed to get the active NO_3^-/NO^+ species in surface reaction with the latter ions. The NO_3^- and methane gives an unidentified intermediate that takes part in a nitrogen forming reaction with NO^+. The activation of methane on active NO_3^- surface species is confirmed to be the rate determining step. The In-bound nitrate has significantly higher reactivity towards methane than Co-bound nitrate, therefore the In-catalysts are more active in the NO-SCR reaction than the Co-catalysts.

The connection between the NO-COX and CH_4/NO-SCR reactions was clearly established. The acceleration of the NO-COX reaction with Co-oxide promoter increases the rate of surface nitrate formation on the In-sites and consequently the rate of methane activation and, as a result, the rate of the NO-SCR reaction. High activity and selectivity are warranted only by the proper balance of the NO-COX and CH_4/NO-SCR activities.

The catalytic functions providing NO-COX and CH_4/NO-SCR activities can be physically separated from each other; however, they are favorably in close proximity, especially at high reaction rates, to avoid that the rate of the NO_2 transport between the active sites of different functions should control the rate of the NO-SCR reaction.

Acknowledgements

The authors thank for the financial support of the Hungarian Research Fund (OTKA no. K-69052). Thanks are also due to the Hungarian-Argentine TéT program (AR-4/08) that made this joint project possible.

References

[1] M. Iwamoto, H. Hamada, Catal. Today 10 (1991) 57–71.
[2] V.I. Parvulescu, P. Grange, B. Delmon, Catal. Today 46 (1998) 233–316.
[3] Y. Traa, B. Burger, J. Weitkamp, Microporous Mesoporous Mater. 30 (1999) 3–41.
[4] R. Burch, J.P. Breen, F.C. Meunier, Appl. Catal. B 39 (2002) 283–303.
[5] Y. Li, J.N. Armor, Appl. Catal. B 1 (1992) L31–L40.
[6] Y. Li, P. Battavio, J.N. Armor, J. Catal. 142 (1993) 561–571.
[7] E. Kikuchi, K. Yogo, Catal. Today 22 (1994) 73–86.
[8] E. Kikuchi, M. Ogura, I. Terasaki, Y. Goto, J. Catal. 161 (1996) 465–470.
[9] M. Ogura, T. Ohsaki, E. Kikuchi, Microporous Mesoporous Mater. 21 (1998) 533–540.
[10] M. Ogura, M. Hayashi, E. Kikuchi, Catal. Today 42 (1998) 159–166.
[11] M. Ogura, M. Hayashi, E. Kikuchi, Catal. Today 45 (1998) 139–145.
[12] J.M. Ramallo-Lopez, F.G. Requejo, L.B. Gutierrez, E.E. Miro, Appl. Catal. B 29 (2001) 35–46.
[13] J.M. Ramallo-Lopez, L.B. Gutierrez, A.G. Bibiloni, F.G. Requejo, E.E. Miro, Catal. Lett. 82 (2002) 131–138.
[14] H. Berndt, F.-W. Schütze, M. Richter, T. Sowade, W. Grünert, Appl. Catal. B 40 (2003) 51–67.
[15] L. Ren, T. Zhang, J. Tang, J. Zhao, N. Li, L. Lin, Appl. Catal. B 41 (2003) 129–136.
[16] A.R. Beltramone, L.B. Pierella, F.G. Requejo, O. Anunziata, Catal. Lett. 91 (2003) 19–24.
[17] T. Maunula, J. Ahola, H. Hamada, Appl. Catal. B 64 (2006) 13–24.
[18] O.A. Anunziata, A.R. Beltramone, F.G. Requejo, J. Mol. Catal. A 267 (2007) 194–201.
[19] R. Serra, M.J. Vecchietti, E. Miro, A. Boix, Catal. Today 133 (2008) 480–486.
[20] A. Kubacka, J. Janas, E. Wloch, B. Sulikowski, Catal. Today 101 (2005) 139–145.
[21] A. Kubacka, J. Janas, B. Sulikowski, Appl. Catal. B 69 (2006) 43–48.
[22] T. Maunula, J. Ahola, H. Hamada, Ind. Eng. Chem. Res. 46 (2007) 2715–2725.
[23] F. Lónyi, H.E. Solt, J. Valyon, H. Decolatti, L.B. Gutierrez, E. Miró, Appl. Catal. B 100 (2010) 133–142.
[24] T. Sowade, T. Liese, C. Schmidt, F.-W. Schütze, X. Yu, H. Berndt, W. Grünert, J. Catal. 225 (2004) 105–115.
[25] I. Halasz, A. Brenner, K.Y. Simon Ng, Y. Hou, Catal. J. 161 (1996) 359–372.
[26] E.M. Holmgreen, M.M. Yung, U.S. Ozkan, Appl. Catal. B 74 (2007) 73–82.
[27] B. Mirkelamoglu, U.S. Ozkan, Appl. Catal. B 96 (2010) 421–433.
[28] K. Hadjiivanov, B. Tsyntsarski, T. Nikolova, Phys. Chem. Chem. Phys. 1 (1999) 4521–4528.
[29] X. Wang, H. Chen, W.M.H. Sachtler, Appl. Catal. B 29 (2001) 47–60.
[30] C. Resini, T. Montanari, L. Nappi, G. Bagnaco, M. Turco, G. Busca, F. Bregani, N. Notaro, G. Rocchini, J. Catal. 214 (2003) 179–190.
[31] G. Bagnasco, M. Turco, C. Resini, T. Montanari, M. Bevilacqua, G. Busca, J. Catal. 225 (2004) 536–540.
[32] L.B. Gutierrez, E.E. Miró, M.A. Ulla, Appl. Catal. A 321 (2007) 7–16.
[33] M. Mhamdi, S. Khaddar-Zine, A. Ghorbel, Appl. Catal. A 357 (2009) 42–50.
[34] H.K. Beyer, R.M. Mihalyi, Ch Minchev, Y. Neinska, V. Kanazirev, Microporous Mater. 7 (1996) 333–341.
[35] R.M. Mihalyi, H.K. Beyer, V. Mavrodinova, Ch Minchev, Y. Neinska, Microporous Mesoporous Mater. 24 (1998) 143–151.
[36] H. Solt, F. Lonyi, R.M. Mihalyi, J. Valyon, J. Phys. Chem. C 112 (2008) 19423–19430.
[37] J.M. Zamaro, E.E. Miró, A.V. Boix, A. Martínez-Hernández, G.A. Fuentes, Microporous Mesoporous Mater. 129 (2010) 74–81.

[38] L. Gutierrez, E.A. Lombardo, Appl. Catal. A 360 (2009) 107–119.
[39] J.A.Z. Pieterse, R.W. van den Brink, S. Booneveld, F.A. de Bruijn, Appl. Catal. B 46 (2003) 239–250.
[40] M.M. Yung, E.M. Holmgreen, U.S. Ozkan, J. Catal. 247 (2007) 356–367.
[41] H. Wang, J. Wang, Z. Wu, Y. Liu, Catal. Lett. 134 (2010) 295–302.
[42] D. Kaucky, A. Vondrova, J. Dedecek, B. Wichterlova, J. Catal. 194 (2000) 318–329.
[43] K. Hadjiivanov, J. Saussey, J.L. Freysz, J.C. Lavalley, Catal. Lett. 52 (1998) 103–108.
[44] F. Lónyi, J. Valyon, L. Gutierrez, M.A. Ulla, E.A. Lombardo, Appl. Catal. B 73 (2007) 1–10.
[45] M.C. Campa, V. Indovina, J. Porous Mater. 14 (2007) 251–261.
[46] E. Ivanova, K. Hadjiivanov, D. Klissurski, M. Bevilacqua, T. Armaroli, G. Busca, Microporous Mesoporous Mater. 46 (2001) 299–309.
[47] T. Weingand, S. Kuba, K. Hadjiivanov, H. Knozinger, J. Catal. 209 (2002) 539–546.
[48] M. Li, Y. Yeom, E. Weitz, M.H. Sachtler, J. Catal. 235 (2005) 201–208.
[49] K.I. Hadjiivanov, Catal Rev.: Sci. Eng. 42 (1–2) (2000) 71–144.
[50] Y. Li, T.L. Slager, J.N. Armor, J. Catal. 150 (1994) 388–399.
[51] L.J. Lobree, A.W. Aylor, J.A. Reimer, A.T. Bell, J. Catal. 169 (1997) 188–193.
[52] K. Hadjiivanov, E. Ivanova, M. Daturi, J. Saussey, J.-C. Lavalley, Chem. Phys. Lett. 370 (2003) 712–718.
[53] K. Gora-Marek, B. Gil, M. Sliwa, J. Datka, Appl. Catal. A 330 (2007) 33–42.
[54] K. Gora-Marek, Top. Catal. 52 (2009) 1023–1029.
[55] F. Geobaldo, B. Onida, P. Rivolo, F. Di Renzo, F. Fajula, E. Garrone, Catal. Today 70 (2001) 107–119.
[56] T. Kanougi, K. Furukawa, M. Yamadaya, Y. Oumi, M. Kubo, A. Stirling, A. Fahmi, A. Miyamoto, Appl. Surf. Sci. 119 (1997) 103–106.
[57] J.J. Kim, C.W. Kim, N.H. Heo, W.T. Lim, K. Seff, J. Phys. Chem. C 114 (2010) 15741–15754.
[58] A.Yu. Stakheev, C.W. Lee, S.J. Park, P.J. Chong, Appl. Catal. B 9 (1996) 65–76.
[59] D.B. Lukyanov, G.A. Sill, J.L. d'Itri, W.K. Hall, J. Catal. 153 (1995) 265–274.
[60] A.D. Cowan, R. Dümpelmann, N.W. Cant, J. Catal. 151 (1995) 356–363.
[61] N.W. Cant, I.O.Y. Liu, Catal. Today 63 (2000) 133–146.